South Asian J. Food Technol. Environ., 6(1): 894-902 (2020)
ISSN 2394-5168 (Print), 2454- 6445(online)
www.sweft.in
DOI: https://doi.org/10.46370/sajfte.2020.v06i01.03

Structured mathematical algorithm for surface temperature estimation based on satellite imagery

Daniel PrakashKushwaha*, Tarate Suryakant Bajirao and Ram Kumar

Department of Soil and Water Conservation Engineering, College of Technology, Govind Ballabh Pant University of Agriculture and Technology, Pantnagar-263145, Uttarakhand, India,
*Email: danielprakash1991@gmail.com

Abstract

Information about surface temperature is essential for agriculture such as growth of vegetation, soil and plant chemical, physical properties, change of climate, glacier melting etc. It combines the results of all surface atmosphere interactions and energy fluxes between the surface and the atmosphere. In this paper, satellite image of 6 Dec 2015 has been used to show the spatial pattern of surface temperature over Udham Singh Nagar district of Uttarakhand state, India. Though land surface temperature derived from satellite, could be a beneficial complement to conventional land surface temperature data sources. This research, proposed a methodology for determining land surface temperature through using a structured mathematical algorithm viz. split window algorithm. Split window algorithm has been used on LANDSAT 8 imagery with operational land imager sensor and thermal infrared sensor. TIRS shows two thermal bands i.e. band 10 and band 11. Split window approach requires brightness temperature value of both band 10 and band 11 along with land surface emissivity which is calculated with the help of operational land imager bands i.e. NIR and Red. The spectral radiance has been determined using thermal infrared bands i.e. band 10 and band 11. Emissivity has been calculated using normalized difference vegetation index threshold technique for which bands 2, 3, 4 and 5 were utilized. At the last step, split window approach uses brightness temperature of two bands of thermal infrared, mean and difference in land surface emissivity for estimating land surface temperature.

Keywords: Split window approach, Fractional vegetation cover, Surface temperature, Udham Singh Nagar.

Paper cited: Kushwaha, D.P., Bajirao, T.S. and Kumar R. (2020). Structured mathematical algorithm for surface temperature estimation based on satellite imagery. *South Asian Journal of Food Technology and Environment,* 6(1): 894-902.

Introduction

Land surface temperature (LST) is very important environmental parameter to be studied. The meaning of land surface temperature is the temperature of earth surface when we directly contact with it. It is also called skin temperature of the earth surface. LST is one of the important factors in global climate change, glacier melting, vegetation growth and soil health. The study of the LST is very crucial in monsoon prone areas. When it rises it causes environmental imbalance situation such as melting in glacier, reduction in vegetation, and change in climatic condition of monsoon areas leading to unpredictable rainfall. The semi-urban areas which are in development stage, are a focal point for social and economic activities and due to which, these are closely related to daily life of human being (Mirzaei and Haghighat, 2010 and Madlener and Sunak, 2011).

Attention is more and more being given to the pursuit of more comfortable living

conditions in semi-urban areas in the face of increasing urbanization. Due to whichour interests are growing in the factors that impact on human ease and wellbeing in cities (Oke, 1982; Quattrochi and Luvall, 1999; Kleerekoper, *et al.,* 2012; Gago, *et al,*. 2013, Santamouris, 2013, Kushwaha, *et al.* 2019 and Xiaokang Kou, *et al,*. 2016). Poor air quality is also responsible for increment in temperature of the earth (Sarrat, *et al.*, 2006) and finally it can boost the energy requirement of an area (Santamouris *et al*., 2001; Kondo and Kikegawa, 2003; Kolokotroni, *et al.*, 2007; Mirzaei and Haghighat, 2010; Kolokotroni *et al.*, 2012 and Ema *et al.*, 2016). Increment in temperature can even contribute to human mortality rates, with thousands of heat-related deaths in every year (Ashley *et al*., 2008 and Gosling *et al.*,2009) and it has been directly linked to adverse impacts on human health (Tan *et al*., 2010 and Cheung and Hart, 2014).

Nowadays, LST is being calculated using satellite imagery containing thermal infrared (TIR) bands (Singh *el al.*, 2018). Therefore with the help of satellite images LST could be a useful complement to traditional LST data sources. TIR remote sensing technique has become one of the important means to study the thermal characteristic of land surface. In this paper, Split window (SW) approach is used to calculate LST. In this study, we have used two thermal bands i.e. band 10 and band 11 in LANDSAT 8 images and we have used moderate resolution LANDSAT 8 bands (30m). During the estimation of LST, we required operational land imager (OLI) sensor bands (which are from band number 2 to band number 5) for determining land surface emissivity (LSE) with the help of fractional vegetation cover (FVC). SW approach combined brightness temperature of band number 10 and11 with LSE to estimate LST for each ground pixels vector.

Materials and methods

Study area and data collection

US Nagar is a famous district of the Uttarakhand state; it is in the tarai region of Kumaon divison. Total geographical area of this district is about three thousand fifty five sq. km. and in aerially it ranks ninth in its own state. It is situated between latitude 28° 53' N to 29° 23' N and and longitudes 78° 45' E to 80° 08' E. The study area falls in survey of India (SOI)Toposheet (Quadrangle Maps) Nos. 53K, O, P and 62D. The overall literacy rate is 64.86%. Agriculture is the primary occupation of the people as it justifies the title of "Chawalki Nagari". About 64% of the total work force involved in farming. Total areas under rabi, khariff and zaid crop are 97973, 139928 and 8580 ha, respectively.

Landsat-8 is one of the Landsat series of NASA. The data of Landsat-8 is available in Earth Explorer website at free of cost. In the present study, the TIR band number 10 and11 were used to estimate brightness temperature and OLI spectral bands 2, 3, 4 and 5 were used to determine normalized difference vegetation index (NDVI). Landsat-8 provides metadata of the bands such as thermal constant, rescaling factor value etc., which can be used for calculating LST. In 2013, the new Landsat series was lunched which is called Landsat data continuity mission (LDCM) or simply Landsat-8. This new generation included the new TIR sensor (TIRS). Its resolution has been given in Table 1. The major difference between the new TIRS and the thematic mapper (TM) or enhanced thematic mapper (ETM) sensors is the existence of two thermal infrared bands in the atmospheric window between10 and 12 µm.

Environment for visualizing images (ENVI) is image processing software and has been used in this study. ENVI combines a number of scientific algorithms, a lot of which are contained in automated, wizard-based approach that walks users through complex tasks. SW approach uses brightness temperature of two bands of TIR, mean and difference in LSE for estimating LST of an area. The SW approach uses the following algorithm;

$$LST = TB_{10} + C_1 (TB_{10}-TB_{11}) + C_2 (TB_{10}-TB_{11})^2 + C_0 + (C_3+C_4e_w) (1- \varepsilon) + (C_5+C_6e_w) \Delta\varepsilon \ldots (1)$$

Where, *LST* is in ^{0}K, fromC_0 to C_6 are split window coefficient values (Skokovic *et. al*., 2014; Sobrino *et al*., 1996; 2003; Zhao *et al*., 2009) given in Table 2, TB_{10} and TB_{11} are brightness temperature in ^{0}K of band 10 and band 11 respectively, ε is mean LSE of TIR bands, e_w is the atmospheric water vapor content (g/cm^3) and $\Delta\varepsilon$ is difference in LSE.

Brightness temperature (T_B): is the microwave radiation radiance traveling upward from the top of Earth's atmosphere. Te calibration process has been done for converting thermal DN values of thermal bands of thermal infrared to T_B. The top of atmospheric (TOA) spectral radiance of ($L\lambda$) was needed for finding T_B of an area. T_B for both the TIR bands was determined by using the following formula;

$$TB = \frac{K_2}{Ln\left\{\left(\frac{K_1}{L\lambda}\right)+1\right\}} \ldots (2)$$

Where, K_1 and K are thermal conversion constant and it varies for both TIR bands, L_λ is TOA spectral radiance and it was determined by multiplying multiplicative rescaling factor (MRF), which is 0.000342, of TIR bands with its corresponding TIR band and adding additive rescaling factor (ARF), which is 0.1, with it.

$$L\lambda = M_L \times Q_{cal} + A_L \ldots (3)$$

Where, $L\lambda$ is in watts per (m^2×srad×μm), M_L is band specific MRF (radiance multi band 10 or 11), Q_{cal} is band 10 or 11 image and A_L is band specific ARF (radiance add band 10 or 11). To find LST it is necessary to calculate the LSE of the region. LSE was estimated using NDVI threshold method and formula is given below;

$$LSE = \varepsilon_s (1-FVC) + \varepsilon_v \times FVC \ldots (4)$$

Where, $\varepsilon_s$and ε_v are the soil and vegetative emissivity values of the corresponding bands. Emissivity values are given in Table 3.

Here FVC was estimated for a pixel and FVC for an image was calculated by;

$$FVC = \frac{NDVI - NDVIs}{NDVIv - NDVIs} \ldots (5)$$

Where, NDVIs is NDVI re-classified for soil NDVIv is NDVI re-classified for vegetation. OLI bands 2, 3, 4 and 5 may be layer stacked and NDVI is estimated using ENVI IP software. The output value of NDVI ranges between -1 and +1, it may vary from one region to other. To get NDVIs and NDVIv, the NDVI image was reclassified into soil and vegetation, the classified data were used to find out FVC. After generating LSE for both the bands of TIR, the mean and difference LSE was found as;

$$\varepsilon = \frac{(\varepsilon 10 + \varepsilon 11)}{2} \ldots (6)$$

$$\Delta\varepsilon = \varepsilon_{10} - \varepsilon_{11} \ldots\ldots (7)$$

Where, ε_{10} and ε_{11} are LSE of band 10 and 11 respectively. Finally, the LST in ^{0}K was determined.

Atmospheric water vapor content (e_w)

Water vapor content of region is the function of Relative humidity (RH). Relative humidity is available at many observatories. In

this study, weather forecasting website *worldweatheronline.com* has been used and got the RH, absolute pressure and temperature of the present day and present time when satellite passed over the region. Although values of the present time RH, absolute pressure and temperature is not available on above mentioned website, so to get the values of the present time RH, absolute pressure and temperature at which study has been performed, interpolation technique has been used and following steps are needed for this;

Equilibrium vapor pressure (e^*_w)

Following formula has been used to determine equilibrium vapor pressure;

$$e_w^* = (1.0007 + 3.46 \times 10^{-6} P) \times (6.1121) e^{\left(\frac{17.502 * T}{240.97 + T}\right)} \ldots. (8)$$

Where, T is the dry bulb temperature expressed in $°C$, P is the absolute pressure in mili-bar and e^*_w is in mili-bar. This formula was given by Buck. Atmospheric water vapor content is measured in hecta-pascal or in mili-bar. To convert it into gram per cube centimeter, a constant 0.098 is multiplied in the mili-bar value of water vapor content. Water vapor content has been calculated using the following relationships;

$$RH = \left(\frac{e_w}{e_w^*}\right) \times 100 \ldots. (9)$$

Table 1: Sensors and their resolutions

Sensor	No. of Bands	Resolution(m)	Path/Row	Date of Acquisition
Operational land imager (OLI)	9	30	145/040	6th Dec 2015
Thermal infrared sensor (TIR)	2	100		

Table 2: Constant values used in split window algorithm

Split window constants	Value
C_0	-0.268
C_1	1.378
C_2	0.183
C_3	54.300
C_4	-2.238
C_5	-129.200
C_6	16.400

Table 3: Emissivity of bands

Emissivity	Band 10	Band 11
ε_s	0.971	0.977
ε_v	0.987	0.989

Results and Discussion

In this study, LST was calculated by applying a SW structured mathematical algorithm and it has been described in earlier methodology. SW uses brightness temperature of TIR band 10, TIR band 11, mean and difference in LSE for estimating LST of an area. The values of thermal conservation constants i.e. K_1 and K_2 and rescaling factors i.e. M_L and A_L have been given in Table 4 and Table 5 respectively for band 10 and band 11 and these values are obtained from the metadata file of the

imagery provided by the image provider website.

To calculate LSE, it is very important to calculate FVC and it is dependent on NDVI of soil as well as of vegetation and its values have been determined by the *Quick Stats* option of the ENVI 4.7 image processing software and given in Table 8. For calculating the value of e_w, we have used the values of RH, absolute pressure and temperature of the day (6th December 2015) and time (10:42:48) when satellite passed over the study area by applying the Equations 2.8 and Equation 2.9 and it has been given in Table 8.

Table 4: Values of thermal conservation constants

Thermal conservation constants	Band 10	Band11
K_1	0774.885	0480.888
K_2	1321.079	1201.144

Table 5: Values of rescaling factor

Rescaling Factor	Band 10	Band 11
M_L	0.000342	0.000342
A_L	0.1	0.1

Table 6: NDVI values for soil and vegetation

NDVI for Soil	0.000993
NDVI for Vegetation	0.354073

Table 7: Calculation for water vapor content (e_w) of the day 6th December 2015 at 10:42:48 of IST

Parameters	Values
Temperature (T) (Recorded)	21 ^{0}C
Relative humidity (RH) (Recorded)	41 %
Absolute pressure (P) (Recorded)	1019 milibar
Equilibrium vapor pressure (e^*_w) (Calculated)	24.965 milibar
Atmospheric water vapor content (e_w)(Calculated)	1.0031 g/cm^3

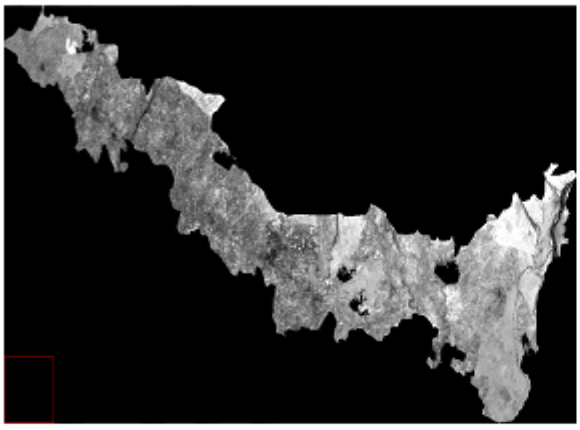

Fig. 1: Spatial pattern of land surface emissivity for band 10

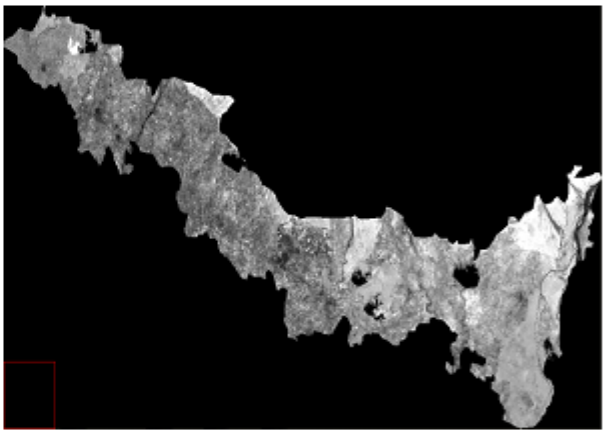

Fig. 2: Spatial pattern of land surface emissivity for band 11

Table 8: Systematic calculations of land surface temperature using split window algoriths

Systematic steps	Parameter	Generalized formula		Formula used in band math of ENVI software	
		Band 10	Band 11	Band 10	Band 11
1	TOA Radiance	3.3420e-4×(B10)+0.1000	3.3420e-4×(B11)+0.1000	3.3420e-4×float(b10)+0.1000	3.3420e-4×float(b11)+0.1000
2	Brightness temp. (TB)	1321.079/alog(774.885/(TOA of B10)+1)	1201.144/alog(480.888/(TOA of B11)+1)	1321.079/alog(774.885/float(TOA of B10)+1)	1201.144/alog(480.888/float(TOA of B11)+1)
3	NDVI	((NIR)-(R))/((NIR)+(R))		(float(b5)-float(b4))/(float(b5)+float(b4))	
4	FVC	((NDVI)-(0.000993))/(0.354073-0.000993))		(float(NDVI)-(0.000993)/(0.354073-0.000993))	
5	LSE	(0.971× (1-(FVC of B10))+0.987× (FVC of B10)	(0.977× (1-(FVC of B11))+0.989× (FVC of B11)	(0.971× (1-float(FVC of B10)))+0.987×float(FVC of B10)	(0.977× (1-float(FVC of B11)))+0.989×float(FVC of B11)
6	Mean of LSE	((LSE of B10)(LSE of B11))/2		(float(LSE of B10)+float(LSE of B11))/2	
7	Difference of LSE	(LSE of B10)-(LSE of B11)		float(LSE of B10)-float(LSE of B11)	
8	LST	((TB for B10)+(1.378× ((TBfor B10)-(TB for B11)))+(0.183× (((TB for B10)-(TB for B11)) × ((TB for B10)-(TB for B11))))-0.268+((54.300+(-2.238×1.0031)) × (1-(Mean of LSE)))+(((-129.2)+16.4×1.0031) × (Diff of LSE)))		(float(TB for B10)+(1.378× (float(TB for B10)-float(TB for B11)))+(0.183× ((float(TB for B10)-float(TB for B11)) × (float(TB for B10)-float(TB for B11))))-0.268+((54.300+(-2.238×1.0031)) × (1-float(Mean of LSE)))+(((-129.2)+16.4×1.0031)×float(Diff of LSE)))	

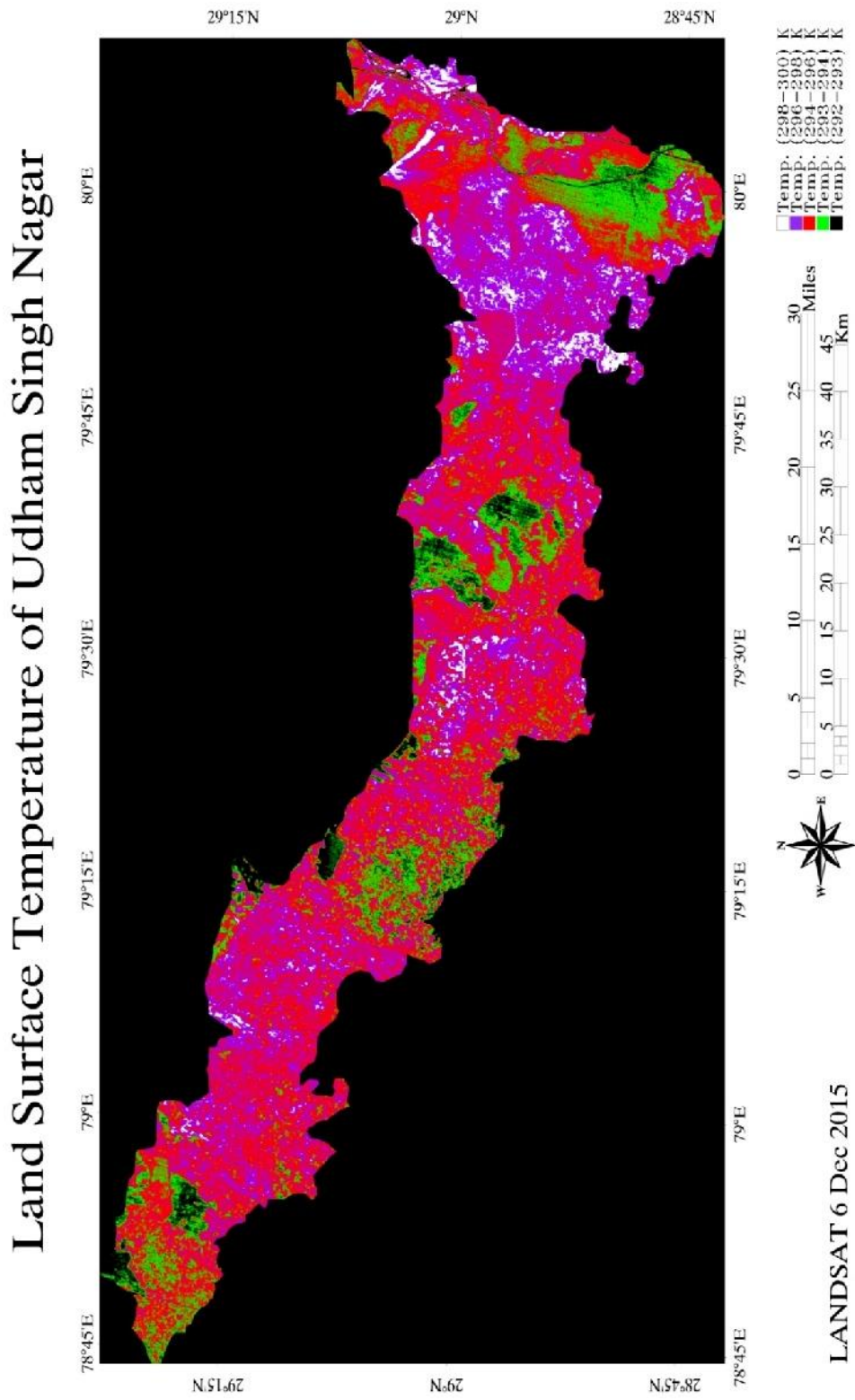

Fig.3: Land surface temperature of Udham Singh Nagar

The flow steps which have been considered to calculate final value of LST in ENVI 4.7 software with the help of TOA radiance, T_B, NDVI, FVC, LSE, mean of LSE and difference of LSE using the Equations 1 through 7 and Tables 3 through 6 have been given systematically in Table 7. Color mapping GREEN-RED-BLUE-WHITE in ENVI software has been used to give the different colors to all the temperature ranges i.e. green, purple, red, white and black to show the LST of different regions of the US Nagar district. LSE for band 10, band 11 of LANDSAT 8(without ENVI color mapping) and LST (with ENVI color mapping) of US Nagar district has been shown in Fig. 1, 2 and 3, respectively.

Conclusions

In this paper, a methodology for retrieving surface temperature by applying a structured mathematical algorithm has been used. Split window approach requires brightness temperature of band 10, band 11 of thermal infrared sensor along with land surface emissivity values which have been calculated using NIR and Red bands. The spectral radiance has also been estimated using TIR bands 10 and 11. Emissivity was calculated with the help of NDVI threshold technique for which OLI bands 2, 3, 4 and 5 have been utilized. This study clearly reveals in regions which have more vegetation cover undergo in low LST values and vice versa. Barren lands, uncultivable land and urban areas experience high LST values. Furthermore, LST has been found high in barren regions and low in hilly regions because of vegetative cover. It was also showed that this approach is easy and suitable in every area to estimate and surface temperature.

Acknowledgements

The authors wish to acknowledge Dr. A. S. Nain, Professor and head, Department of Agro-meteorology, GBPUAT, Pantnagar for providing laboratory facilities and useful guidance. Authors are also thankful to his college teachers and seniors for providing support and help for this work.

References

1. Ashley, E. and Lemay, L. (2008). Concrete's contribution to sustainable development, from http://www.specifyconcrete.org/assets/docs/ Concretes 20%Contribution to Sustainable Development.pdf.
2. Cheung, C. and Hart, M. (2014). Climate change and thermal comfort in Hong Kong. *International Journal of Biometeorology*, 58(2): 137–148.
3. Ema, K., Nengah, S.J. and Widiatmaka. (2016). Satellite-Based Land Surface Temperature Estimation of Bogor Municipality, Indonesia. *Indonesian Journal of Electrical Engineering and Computer Science*, DOI: 10.11591/ijeecs.v2.i1, 2 (1): 221-228.
4. Gago, E.J., Roldan, J., Pacheco-Torres, R. and Ordonez, J. (2013). The city and urban heat islands: A review of strategies to mitigate adverse effects. *Renewable and Sustainable Energy Reviews*, 25: 749–758.
5. Gosling, S., Lowe, J., Mc-Gregor, G., Pelling, M. and Malamud, B. (2009). Associations between elevated atmospheric temperature and human mortality: A critical review. *Climatic Change*, 92(3–4): 299–341.
6. Kleerekoper, L., Van-Esch, M. and Salcedo, T.B. (2012). How to make a city climate-proof, addressing the urban heat is land effect. *Resources, Conservation and Recycling*, 64: 30–38.
7. Kolokotroni, M., Ren,X., Davies, M. and Mavrogianni, A. (2012). London's urban heat island: Impact on current and future energy consumption in office buildings. *Energy and Buildings*, 47: 302–311.
8. Kolokotroni, M., Zhang, Y. and Watkins, R. (2007). The London Heat Island and building cooling design. *Solar Energy*, 81(1): 102–110.

9. Kondo, H. and Kikegawa, Y. (2003). Temperature variation in the urban canopy with anthropogenic energy use. *Pure and Applied Geophysics*, 160(1–2): 317–324.
10. Kushwaha, D.P., Malik, A. and Singh, S.K. (2019). Geographic information system for generating spatial pattern of natural streams: A case study in Nainital, India. *Bulletin of Environment, Pharmacology and Life Sciences*, 8 (2): 56-63.
11. Madlener, R. and Sunak, Y. (2011). Impacts of urbanization on urban structures and energy demand: What can welearn for urban energy planning and urbanization management. *Sustainable Cities and Society*, 1(1): 45-53.
12. Mirzaei, P.A. and Haghighat, F. (2010). Approaches to study Urban Heat Island, Abilities and limitations. *Building and Environment.* 45(10): 2192–2201.
13. Oke, T.R. (1982). The energetic basis of the Urban Heat-Island. *Quarterly Journal of the Royal Meteorological Society*, 108(455): 1–24.
14. Quattrochi, D.A. and Luvall, J.C. (1999). Thermal infrared remote sensing for analysis of landscape ecological processes: Methods and applications. *Landscape Ecology*, 14(6): 577–598.
15. Santamouris, M. (2013). Using cool pavements as a mitigation strategy to fight urban heat island—A review. *Solar Energy*, 82(1): 301–312.
16. Santamouris, M., Papanikolaou, N., Livada, I., Koronakis, I., Georgakis, C. and Argiriou, A. (2001). On the impact of urban climate on the energy consumption of buildings, *Solar Energy*, 70(3): 201–216.
17. Sarrat, C., Lemonsu, A., Masson, V. and Guedalia, D. (2006). Impact of urban heat island on regional atmospheric pollution. *Atmospheric Environment*, 40(10): 1743–1758.
18. Singh, V.K., Singh, B.P., Kisi, O. and Kushwaha, D.P. (2018). Spatial and multi-depth temporal soil temperature assessment by assimilating satellite imagery, artificial intelligence and regression based models in arid area. *Computers and Electronics in Agriculture*, 150: 205–219.
19. Skokovic, D., Sobrino, J.A., Jimenez-Munoz. J.C., Soria. G., Julien. Y., Mattar, C. and Jordi Cristobal (2014). Calibration and Validation of Land Surface Temperature for Landsat 8 – TIRS Sens. *Land product Validation and Evolution*, ESA/ESRIN Frascati (Italy): 6-9, January 28-30,.
20. Sobrino, J.A., Li, Z.L., Stoll, M.P., Becker, F. (1996). Multi-channel and multi-angle algorithms for estimating sea and land surface temperature with ATSR data. *International Journal Remote Sensing*, 17: 2089–2114.
21. Tan, J., Zheng, Y., Tang, X., Guo, C., Li, L., Song, G. (2010). The urban heat island and its impact on heat waves and human health in Shanghai. *International Journal of Biometeorology*, 54(1): 75–84.
22. Xiaokang Kou, L.J., Yanchen, B., Shuang, Y. and Linna, C. (2016). Estimation of Land Surface Temperature through Blending MODIS and AMSR-E Data with the Bayesian Maximum Entropy Method. *Remote sensing*, 108(5): 1-17, DOI: 10.3390/rs8020105.
23. Zhao, S., Qin, Q., Yang, Y., Xiong, Y. and Qiu, G. (2009). Comparison of two Split-Window Methods for Retrieving Land Surface Temperature from MODIS Data. *Journal of Earth System Science*, 118(4): 345- 353.

Received	: February, 2020
Revised	: April, 2020
Published	: June, 2020